AN INNOVATIVE MECHANICAL AND CONTROL ARCHITECTURE FOR A BIOMIMETIC HEXAPOD FOR PLANETARY EXPLORATION

M. Pavone*, P. Arena§ and L. Patané§

*Scuola Superiore di Catania,
Via S. Paolo 73, 95123 Catania, Italy
§Dipartimento di Ingegneria Elettrica Elettronica e dei Sistemi,
Università degli Studi di Catania, Viale A. Doria, 6 - 95125 Catania, Italy

Abstract— **This paper addresses the design of a six legged robot for planetary exploration. The robot is specifically designed for uneven terrains and is biologically inspired on different levels: mechanically as well as in control. A novel structure is developed basing on a (careful) emulation of the cockroach, whose extraordinary agility and speed are principally due to its self-stabilizing posture and specializing legged function. Structure design enhances these properties, in particular with an innovative piston-like scheme for rear legs, while avoiding an excessive and useless complexity. Locomotion control is designed following an analog electronics approach, that in space applications could hold many benefits. In particular, the locomotion control is based on a Cellular Neural Network playing the role of an artificial Central Pattern Generator. Several dynamical simulations were carried out to test the structure and the locomotion control. Simulation results led to the implementation of the first prototype: Gregor I. Experimental tests showed that Gregor I is able to walk at the travel speed of 0.1 body length per second and to successfully negotiate obstacles more than 170% of the height of robot's mass center.**

I. INTRODUCTION

The recent planetary explorative missions as well as the scheduled ones for the next years put in light the necessity, for planetary unmanned missions, of using autonomous mobile platforms.

Mechanical structure is the first issue to be addressed. Possible mechanisms capable of producing locomotion are: wheels, caterpillar treads and legs. Wheeled and tracked robots are much easier to design and to implement if compared with legged robots and led to successful missions like *Mars Pathfinder* or *Spirit and Opportunity*; nevertheless, they carry a set of disadvantages that hamper their use in more complex explorative tasks. Firstly, wheeled and tracked vehicles, even if designed specifically for harsh terrains, cannot maneuver over an obstacle significantly shorter than the vehicle itself; a legged vehicle, on the other hand, could be expected to climb an obstacle up to twice its own height, much like a cockroach can. Secondly, wheeled and tracked vehicles are also inherently less robust than those dependent on legs. The loss of a single leg on a hexapod will result in only minimal loss in maneuverability, *i.e.* in a *mechanical graceful degradation*; on a wheeled vehicle a damaged wheel could spell the end of mobility, and a damaged caterpillar tread almost always results in catastrophic failure. Finally, legged vehicles are far more capable of navigating an intermittent substrate -such as a slatted surface- than wheeled or tracked vehicles [1].

That is why the concept of a fully autonomous, mission capable, legged robot is acquiring an ever increasing interest in the field of space explorative robotics.

Given the preceding arguments for the use of legged locomotion in certain environments, one is left with the daunting task of actually designing an efficient locomotion control for legged robots. The basic consideration is that legged structures have a great number of degrees of freedom, to be controlled concurrently.

In this paper we describe the design of a six-legged robot aimed at space explorative missions. Strongly believing that a bio-inspired approach can largely benefit the design of an autonomous legged robot, we took explicitly inspiration from cockroach experimental observations. Biological results inspired both the hexapod structure and the control system architecture.

In order to replicate at least in part cockroach's extraordinary agility, each of the three leg pairs has

* Corresponding author. *Mail*: `mapavone@ssc.unict.it`

a unique design: front legs and middle legs have 3 degrees of freedom and a kind of pantograph mechanism aimed at facilitating obstacle climbing task, while rear legs have 2 degrees of freedom and a piston-like design suitable for powerful forward thrusting. Our main concern is on the mechanics of rear legs, that seem to play a crucial role in obstacle overcoming and payload capability. Moreover Gregor I exhibits a *sprawled posture*, able to guarantee a statically stable posture and thus a high margin of stability [2]. Dynamical simulations and experimental tests prove that, thanks to the careful linear/rotational actuation and to the sprawled posture, Gregor I is able to successfully negotiate obstacles of considerable height.

The methodology adopted in this paper for legged locomotion control took its inspiration from the biological paradigm of Central Pattern Generator (CPG) [3] and was firstly outlined in [4]. In insects, the activation of the appropriate muscles in the legs and their coordination take place locally by means of groups of neurons functionally organized in CPG modules. The basic units of the adopted artificial CPG are here nonlinear oscillators coupled together to form a network able to generate a pattern of synchronization that is used to coordinate the robot actuators. Cellular Neural Network (CNN) paradigm, introduced in [5], provides a framework for the implementation of these nonlinear oscillators: each oscillator is simply viewed as a cell of a CNN. This technique has been previously used to control the locomotion of several different bio-inspired robotic structures: simple hexapods, octopods and lamprey-like robots [6], [7]; here this technique is extended to the control of an hexapod in which each leg pair has a unique design. A direct VLSI realization of the control system is possible: a chip for locomotion control implemented by a CNN-based CPG is introduced in [8].

This approach, thanks to its intrinsic modularity, allows an arbitrarily large number of actuators to be controlled concurrently and thus is particularly suitable for legged locomotion control. Further advantages are ease of implementation, robustness and flexibility.

The implementation itself is advantageous since it just involves analog electronics. In space applications, analog circuitry could hold many benefits. Analog circuits provide a very high bandwidth sensor-to-motor signal transformation and avoid any time-consuming conversion between analog and digital signals; thus analog circuits allow actuator outputs to be rapidly modulated in response to sensor feedback, as needed for autonomous planetary explorers. Most importantly, analog circuitry appears to be more robust against space radiation. For example, Single Event Upset (SEU) (*i.e.* radiation-induced errors in microelectronic circuits caused when charged particles lose energy by ionizing the medium through which they pass) in analog circuitry just causes a graceful degradation in performance, while in digital circuitry can cause bit flips and therefore result in catastrophic failures by placing the device into a test mode, halt, or undefined state [9].

This paper is organized as follows. In Section II we discuss basic biological observations in insects and we review some previous hexapods in literature. Then, in Section III we describe the physical design, while in Section IV we discuss the locomotion control. Simulation results follow in Section V. In Section VI we show the physical implementation and, finally, in Section VII we draw our conclusions.

II. BIOLOGICAL INSPIRATION AND LITERATURE REVIEW

Gregor I design is based on biological observations in insects. In this section, firstly we outline some of the most important results coming from insect experimental observations, with particular emphasis on the cockroach *Blaberus Discoidalis*. Then, we review some previous hexapods in literature.

A. *Structure of Blaberus Discoidalis*

Most important structural features of *Blaberus Discoidalis* from an engineering viewpoint are:
- leg structure;
- leg articulation;
- body structure.

Each cockroach leg is divided into several segments. The leg segments from the most proximal to the most distal segment are called coxa, trochanter, femur, tibia and tarsus; the last one is indeed constituted by a series of foot joints.

The complex musculature coupled with complex mechanics confers upon the joint between body and coxa three degrees of freedom (DOF), much like that of a ball and socket joint. The joints between the coxa and trochanter, between the trochanter and femur, and between the femur and tibia are, instead, simple one DOF rotational joints. The joint between the trochanter and femur makes only a small movement and has often been referred to as fused. Each tarsal joint has several passive DOF, guaranteeing agile foot placement. Finally, a claw located on the end of the

tarsus can be raised or lowered to engage the substrate during locomotion on slippery surfaces for climbing [10].

Although the segments are reproduced in each of the three pairs of legs, their dimensions are very different in the front, middle and rear legs. Therefore, front, middle and rear legs are different in length, yielding a ratio of front:middle:rear leg lengths of 1:1.2:1.7 [11]. Leg pairs with different length provide agility and adaptability. Cockroach legs articulate differently with the body, with the front legs oriented almost vertically at rest and middle and rear legs angled posteriorly of about $30°$ and $50°$ respectively [11]. This configuration confers a *sprawled posture* able to guarantee a statically stable posture and thus a high margin of stability [2], [12]. Finally, body is divided into three articulated segments called pro-thoracic, mesothoracic and metathoracic segments. Anyway, dorsal flexion is seldom accomplished [13].

Legs perform different functions [13]:

- **Front legs** – are mainly used to push the body of the cockroaches over obstacles. They also play an important role in turning and in decelerating.
- **Middle legs** – act to push the cockroaches forward but also push the body of the cockroaches over obstacles.
- **Rear legs** generate the major part of the forward motion. They push directly toward the mass center and the contact point is far behind to prevent the cockroaches falling on their back when climbing obstacles.

B. *CPG and locomotion gaits*

Most insects exhibit a hierarchical locomotion control and use a modular organization of the control elements. The activation of the appropriate muscles in the legs and their coordination take place locally by means of groups of neurons functionally organized in modules called Central Pattern Generators (CPG). The output signals of the CPG control directly the effector organs. Distinct periodic patterns of leg movements, called gaits, are due to patterns of neural activity within the CPG [14]. The CPG receives stimuli from the high level control layers that monitor overall locomotion and take decisions about the high level task for example by changing the locomotion gait.

Three different gaits are typically shown by hexapods during walking: fast, medium and slow gait. They are adopted under different conditions to perform high speed locomotion (fast gait) or extremely stable and secure movements (slow gait).

The characteristics of these locomotion gaits can be rigorously defined through the concepts of *cycle time*, *duty factor*, and *leg phases*. The cycle time is the time required for a leg to complete a locomotion cycle. The duty factor df_i is the time fraction of a cycle time in which the leg i is in the power stroke phase. The leg phase φ_i is the fraction of a cycle period by which the beginning of the return stroke of leg i lags behind the beginning of the return stroke of the left front leg (L1), chosen as a reference. Basing on these quantities, a precise gait classification is shown in Tab. I:

TABLE I
CLASSIFICATION OF FAST, MEDIUM AND SLOW GAITS

Fast	Medium	Slow
$\varphi_{L2} = \frac{1}{2}$	$\varphi_{L2} = \frac{3}{4}$	$\varphi_{L2} = \frac{4}{6}$
$\varphi_{L3} = 0$	$\varphi_{L3} = \frac{2}{4}$	$\varphi_{L3} = \frac{2}{6}$
$\varphi_{R1} = \frac{1}{2}$	$\varphi_{R1} = \frac{2}{4}$	$\varphi_{R1} = \frac{3}{6}$
$\varphi_{R2} = 0$	$\varphi_{R2} = \frac{1}{4}$	$\varphi_{R2} = \frac{1}{6}$
$\varphi_{R3} = \frac{1}{2}$	$\varphi_{R3} = 0$	$\varphi_{R3} = \frac{5}{6}$
$df_i = 1/2$	$df_i = 5/8$	$df_i = 9/12$

C. *Hexapod robots in literature*

Major issues involved in hexapod robots' design are:

- leg design;
- actuator selection;
- locomotion control.

First question to be addressed in leg design is the number of degrees of freedom that each leg should possess: many DOF imply better agility and flexibility, but a more difficult control. An example of robot with just one DOF per leg is Rhex [15]. Robot structure consists of a rigid body with six equal compliant legs, each possessing only one independently actuated revolute degree of freedom. The attachment points of the legs as well as the joint orientations are all fixed relative to the body. Basically, spoked wheel concept is exploited. This very simple design guarantees surprisingly good locomotion properties, but lacks of the agility needed for more complex tasks.

Several hexapod robots reported in literature have legs with 2 DOF; one example is Sprawlita [12]. Sprawlita has 6 identical legs with 2 degrees of freedom each. The primary thrusting action in Sprawlita is performed by a prismatic actuator, implemented by a pneumatic piston. This piston is attached to the body through a compliant rotary joint at the hip.

This unactuated rotary joint is based on studies of the cockroachs compliant trochanter-femur joint, which, as stated above, is largely passive. In the prototype, the compliant hip joint allows rotation mainly in the sagittal plane. These active-prismatic, passive-rotary legs are sprawled in the sagittal plane to provide specialized leg function (although all legs are indeed identical). Servo motors rotate the base of the hip with respect to the body, thus setting the nominal, or equilibrium, angle about which the leg will rotate. By changing this angle, the function that the leg performs is affected; *e.g.* aiming the thrusting action towards the back, robot accelerates, on the contrary towards the front robot decelerates. Sprawlita is fast and able to negotiate small obstacles, but can not perform more complex tasks due to the lack of legs' kinematic dexterity.

Another interesting example is Boadicea [16]; its legs use a 2 dimensional pantograph mechanism that produces linear foot motions, with the advantage of simpler software control. A second advantage of the pantograph mechanism is that it provides a large leg workspace with a relatively simple and compact mechanism. Like an insect, Boadicea has different front, middle, and rear legs.

An example of robot with 3 DOF per leg is UIUC, discussed in [11]. Legs are divided into three segments, corresponding to the three main segments of insect legs: coxa, femur, and tibia. The coxa articulates with the body, the femur with the coxa, and the tibia with the femur. Each of the joints between leg segments and between the coxa and the body is a simple hinge joint. The length ratio for the robot's legs is 1 : 1.1 : 1.5. The coxae of the front legs are attached vertically, while the middle leg coxae are attached at an angle of about $75°$ from horizontal. Finally, rear legs are attached at an angle of about $30°$. This structure, taking into account the most important features of a cockroach, confers to the robot a high stability and avoids a useless complexity.

An hexapod robot kinematically similar to *Blaberus Discoidalis* is Robot V, discussed in [1]. Rear legs have three DOF, middle legs have four DOF and front legs have five DOF. Leg design attempts to capture in detail all cockroach leg features, but the resulting robot is more useful from a theoretical than from a practical viewpoint due to its complexity.

Actuator selection represents a fundamental issue in robot design, since the shape, size, weight and strength of an actuator and its power source provide the greatest constraint on robot's potential abilities. Biological organisms have a great advantage over mechanical systems in that muscles, the biological actuators, have a favorable power-to-weight ratio and require low levels of activation energy, compared to any actuator [1].

The most frequently used actuators are electric motors and pneumatic/hydraulic cylinders. Electric motors are the most commonly used actuators since they are readily available in a wide range of sizes and are very easy to control and integrate in a hardware scheme. However, electric motors have some disadvantages: they can provide just a rotational motion and, most importantly, they have a low power-to-weight ratio. On the contrary, pneumatic and hydraulic actuators have a high power-to-weight ratio and produce linear motion. Unfortunately, pneumatic/hydraulic cylinders are better suited to "bang-bang" operations, need a complex mechanics and require a sophisticated control; furthermore, pneumatic actuators need an expensive and heavy compressor. Recently, many new types of actuators are being introduced like Shape Memory Alloys, Piezoelectric Motors and Electroactive Polymers. In [17] the feasibility of a worm-like robot actuated by IPMC is discussed.

Referring to previous robots, RHex is electrically actuated, Sprawlita, Boadicea and UIUC are pneumatically actuated, Robot V is actuated by means of McKibben artificial muscles.

III. PHYSICAL DESIGN

Biological principles and previous hexapod prototypes guided the structure design phase. Our main concern was to replicate the cockroach features that are mainly responsible of its extreme agility, adaptability and stability. We also took into careful consideration fundamental engineering issues like actuator selection.

Before the structure design is started, it is necessary to specify what Gregor I is intended to do, since the final task deeply affects the overall design: *e.g.*, as far as leg design is concerned, if the focus is just on horizontal walking, two DOF per leg are enough. The goals of Gregor I include efficiently walking on uneven terrains and climbing over obstacles whose height is at least equal to robot center of mass (CoM) height, as well as payload capability.

In this section, we outline the various steps that led to the final robot structure, from leg design to overall structure. Our major concern here was on the design of rear legs (that seem to play a crucial role in obstacle climbing and payload capability), and on center of mass placement.

A dynamic robot model was built in a C++ environment basing on `DynaMechs` libraries [18]. Dynamical simulation of the model allowed us to assess structure and control suitability, as it will be discussed in section V.

A. *Front and middle legs*

Front legs have to provide enough flexibility to guarantee an efficient obstacle approach and an effective postural control. Toward this end, front legs are divided into three segments (analogous to coxa, femur and tibia), articulated through 3 DOF rotational joints (α, β and γ joints in Fig. 1); in Fig. 1, rotation axes are depicted. These rotational joints clearly require a precise control, but they do not need high actuation torques, therefore they can be actuated by conventional electrical motors.

As far as mechanical details are concerned, all segments are simply modelled as cylinders whose weights are reported in Tab. II together with the physical dimensions (radius and height respectively).

TABLE II
COXA, FEMUR AND TIBIA PROPERTIES FOR FRONT AND
MIDDLE LEGS

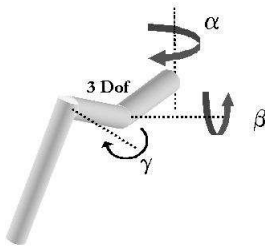| Segment	Weight g	Dimensions cm
Coxa	50	0.5×3
Femur	50	0.5×3
Tibia	30	0.5×6

Fig. 1.   Front leg structure (not in scale).

Middle leg design is identical to front leg design except for the α axis (Fig. 2); this change allows middle legs to efficiently provide part of the forward thrust.

As far as dynamics is concerned, both in front and middle legs joint α allows leg forward movement, joint β allows raising movement and, finally, joint γ guarantees roll and pitch angle control. The γ joint plays a fundamental role in the attitude control, but is not needed for basic locomotion; therefore, as far
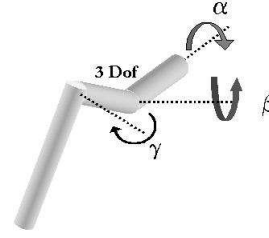

Fig. 2.   Middle leg structure (not in scale).

as basic locomotion is concerned, γ joint is kept at the constant value 0.5 rad from the vertical.

B. *Rear legs*

In rear leg design we bring the most important innovation as far as robot structure is concerned. Since main function of rear legs is powerful thrust, we considered a robust and compact design that could allow the use of a "bang-bang" pneumatic actuation.

Rear legs are divided into two segments (coxa and tibia respectively); coxa segment is articulated with the body with a rotational joint (α joint), while the coxa-tibia joint is prismatic (d joint), as shown in Fig. 3; α joint provides forward movement, while the d joint provides raising movement. Thus, rear legs possess a peculiar hybrid linear/rotational actuation that could allow the use of a combination of electrical and pneumatic actuators.

Rear legs are considerably longer in order to facilitate obstacle climbing. Both segments are simply modelled as cylinders whose weights and dimensions are reported in Tab. III.   As far as dynamics is

TABLE III
REAR COXA AND TIBIA PROPERTIES

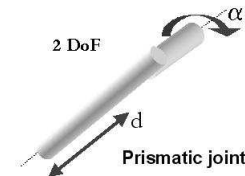| Segment	Weight g	Dimensions cm
Coxa	50	0.5×1
Tibia	80	0.5×12

Fig. 3.   Rear leg structure (not in scale).

concerned, joint α allows leg forward movement and joint d allows raising movement.

C. *Body and payload*

Body is modelled by just one segment with parallelepiped shape; we also considered the presence of a payload, similarly modelled as a parallelepiped (dark part in Fig. 4). Weights and dimensions are reported in Tab. IV and Tab. V.

TABLE IV
BODY PROPERTIES

Mass g	Length cm	Width cm	Height cm
260	30	8	3

TABLE V
PAYLOAD PROPERTIES

Mass g	Length cm	Width cm	Height cm
50	9	5	2

D. *Overall structure*

In order to confer a sprawled posture with a pitch angle of $\varphi \simeq 20°$, legs articulate differently with the body; articulation angles between leg and body are shown in Tab. VI.

TABLE VI
LEG ANGLES FROM HORIZONTAL AT REST

Front legs	90°
Middle legs	60°
Rear legs	20°

Position of the CoM of the fully assembled robot is critical for good performance, as observed in several simulations. Therefore, we studied in detail payload placement through an iterative process. Assuming a body reference system with the z-axis aligned along the body longitudinal axis and the origin located at the body mass center, we finally placed the payload mass center at the coordinate, along the z-axis, -4 cm. With this arrangement, CoM of the overall robot is placed across the dorsal-abdominal part. Simulations proved that in this way speed and stability are enhanced.

The overall structure is shown in Fig.4 (dark part represents the payload), where the sprawled posture, the peculiar leg articulation and the payload placement are evident.

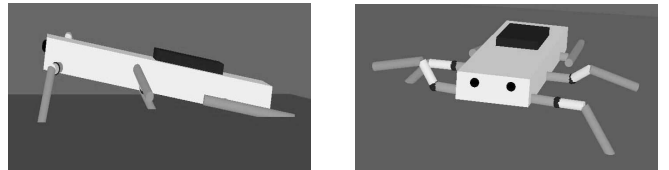Overall, robot weight is 1090 g and robot CoM height is 4 cm.

Fig. 4.   Overall structure: side view and front view.

IV. LOCOMOTION CONTROL: CNN-CPG AND LEG DYNAMICS

As stated above, Gregor I locomotion control takes its inspiration from the biological paradigm of Central Pattern Generator. The basic units of the adopted artificial CPG are nonlinear oscillators coupled together to form a network able to generate a pattern of synchronization that is used to coordinate the robot actuators. In particular, the dynamics of each oscillator can be efficiently exploited to control the leg kinematics of an insect-like hexapod robot by carefully mapping oscillator limit cycles in the limit cycles performed by legs in the joint space.

Cellular Neural Network paradigm provides a framework for the implementation of these nonlinear oscillators: each oscillator is simply viewed as a cell of a CNN.

The following equations describe the nonlinear oscillator (CNN cell) acting as a neuron of the artificial CPG:

$$\begin{cases} \dot{x}_1 = k(-x_1 + (1 + \mu)y_1 - sy_2 + i_1 + \sum_s I_{1,s}) \\ \dot{x}_2 = k(-x_2 + sy_1 + (1 + \mu)y_2 + i_2 + \sum_s I_{2,s}) \end{cases} \quad (1)$$

where $y_i = \frac{1}{2}(|x_i + 1| - |x_i - 1|)$ with $i = 1, 2$. The terms $\sum_s I_{1,s}$ and $\sum_s I_{2,s}$ represent the sum of all the synaptic inputs coming from the other neurons, *i.e.* represent the interconnection with the other neurons. For the choice of the parameters given in Tab. VII, system (1) admits a periodic solution with slow-fast dynamics (in particular the outputs y_1 and y_2 perform a unitary and square-shaped limit cycle): these regular oscillations provide the rhythmic movements for the robot actuators.

TABLE VII
CNN PARAMETERS

μ	s	i_1	i_2	k
0.5	1.2	-0.3	0.3	$\frac{10}{3}$

During a step, legs perform in the joint space a limit cycle, therefore it is natural to map the oscillator dynamics into the leg dynamics through suitable transformation functions. To coordinate the

movements it is necessary to properly synchronize the CPG neurons. This can be done by establishing suitable connections among the nonlinear oscillators, as discussed in [19], where this approach is applied to a robot equipped with 6 identical legs.

Gregor I actuation is more complex, since each leg pair has a unique design; anyway it is still possible to adopt a CNN-CPG with identical cells, basing on the following considerations. As far as basic locomotion is concerned, we can just actuate the α and β joints in front and middle legs and α and d joints in rear legs, since the γ joint actuation is needed just for postural adjustments. The key point is that, although different, legs have to perform similar limit cycles in the joint space (alternating forward and raising movement).

Thus, we can still consider, through *ad hoc* transformations, a mapping between CNN cell limit cycles and leg limit cycles.

In detail, Gregor I CPG is composed by six neurons (1), each one controlling through its two outputs y_2 and y_1 a leg (respectively: the α and β joints in front and middle legs and α and d joints in rear legs). The CNN outputs do not directly control the actuators; they instead undergo a two stages transformation in order to fit the peculiar leg design.

In the first stage, the identical and unitary limit cycles performed by CNN cells are mapped through the maps Z_{front}, Z_{middle} and Z_{rear} into three different unitary limit cycles. These transformations are graphically shown in Fig. 5. After this stage, the following new outputs for front, middle and rear legs are obtained:

$$\zeta_i^{front} = Z_{front}\left(y_i^{front}\right)$$
$$\zeta_i^{middle} = Z_{middle}\left(y_i^{middle}\right)$$
$$\zeta_i^{rear} = Z_{rear}\left(y_i^{rear}\right)$$

The range of motion of each DOF is just as important as the number of DOF in the legs and their basic dynamic. Therefore in a second stage the new outputs are differently scaled and biased in order to achieve suitable range of motion:

$$\alpha_{front} = a_{front}\zeta_2^{front}$$
$$\beta_{front} = b_{front}\zeta_1^{front}$$
$$\alpha_{middle} = a_{middle}\zeta_2^{middle}$$
$$\beta_{middle} = b_{middle}\zeta_1^{middle}$$
$$\alpha_{rear} = a_{rear}\zeta_2^{rear}$$
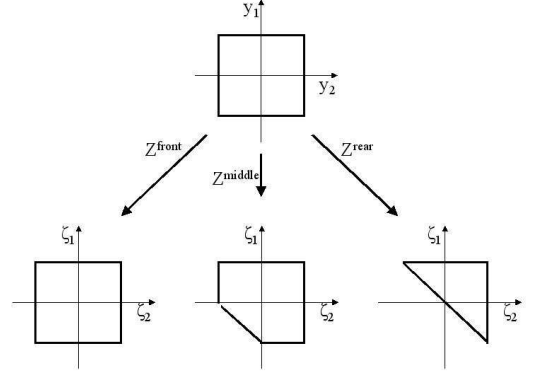$$d_{rear} = b_{rear}\zeta_1^{rear}$$

Fig. 5.   CPG signals transformation.

Scaling and biasing factors were selected basing on simulation performance results and physical feasibility. Actuation parameters are shown in Tab. VIII.

TABLE VIII
ACTUATION PARAMETERS

a_{front}	b_{front}	a_{middle}	b_{middle}	a_{rear}	b_{rear}
0.45 rad	0.9 rad	0.4 rad	0.7 rad	0.15 rad	6 cm

Synchronization is achieved through suitable connections among the neurons depending on the adopted gait, as discussed in [19]. In particular we considered a fast gait and therefore the synaptic connections depicted in Fig. 6. A synaptic connection of strength ϵ from neuron i to neuron j (represented by a line terminating with a dot next to neuron j) adds to the first layer inputs of neuron j the output of the first layer of neuron i times ϵ; in particular $\varepsilon = -0.6$, *i.e.*, synapses are inhibitory.
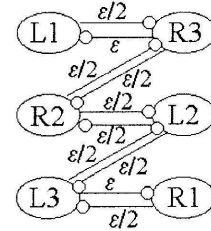

Fig. 6.   CPG neuron connections.

V.   **SIMULATION RESULTS**

The dynamic robot model was tested in a C++ environment based on `DynaMechs` library [18]. The library efficiently simulates the dynamics of robotic articulations and provides a comfortable framework

to translate in C++ the control system architecture. The overall C++ program is available upon request.

The outputs from the simulation include the joint torques, the body motions and the ground reaction forces. The body motions of the model are not inputs and therefore are a good measure of the success of the simulation. The joint torques are used in robot design to size actuators.

A. Environmental properties

Environmental properties to be set are: Ground Normal Spring Constant k_N, Ground Planar Spring Constant k_P, Ground Normal Damper Constant γ_N, Ground Planar Damper Constant γ_P, Coefficient of Static Friction μ_s, Coefficient of Kinetic Friction μ_d and Gravity Acceleration.

Spring and damper constants are used to define how the robot interacts with the surface. The values chosen for Gregor I are typical values for a hard terrain.

Coefficient of Static Friction and Coefficient of Kinetic Friction model sliding across the surface. The chosen values for friction parameters are typical values for a normal terrain. All values are shown in Tab. IX. Gravity acceleration was set at 9.81 m/s^2.

TABLE IX
TERRAIN PROPERTIES

k_N g/s^2	k_P g/s^2	γ_N g/s	γ_P g/s	μ_s	μ_d
75000	75000	2000	2000	1.5	1

B. Integration algorithm

Runge-Kutta of 4th Order was selected for Gregor I simulation as it provides a good numerical approximation with acceptable computational overhead. A step size of 10^{-4} s was found to be appropriate for Gregor I simulation, as values larger than this may cause the controller to become unstable. All simulations were conducted on a 2.8 GHz Pentium class machine, running Microsoft Windows XP. On this machine, 2.8 seconds of dynamical simulation correspond to 10 seconds of computer computation.

C. Simulation experiments

We tested the structure functionality and stability in two conditions: horizontal walking and obstacle climbing. We also studied the maximum achievable payload in presence of actuators able to deliver 11 Kgf · cm. Our main focus was on the determination of the joint torques in order to size actuators. The
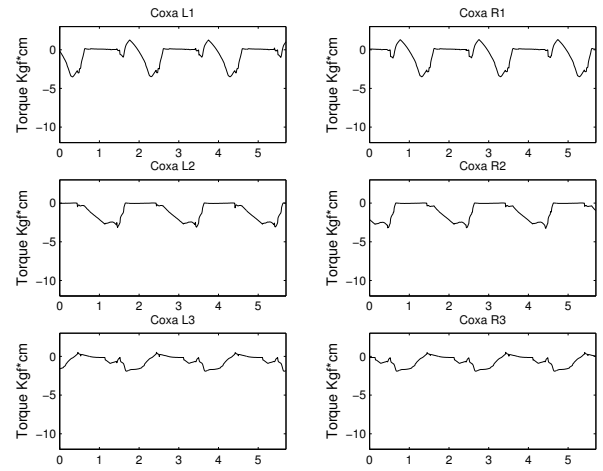

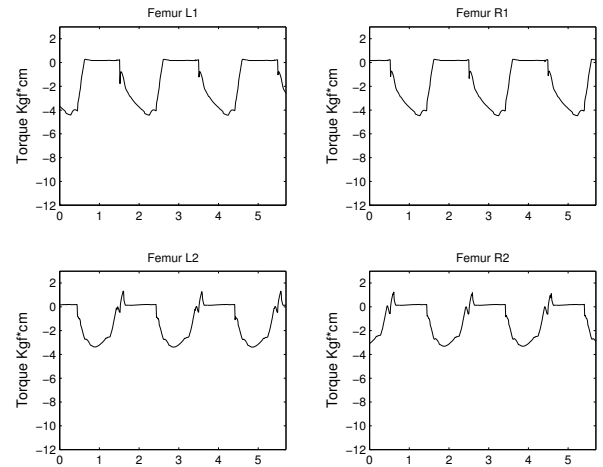Fig. 7. Coxa torques during walking (on the x-axis time in seconds is shown).

Fig. 8. Femur torques during walking (on the x-axis time in seconds is shown).

model has a total of 22 DOF: three translations and three rotations of the body, three DOF in front and middle legs and two DOF in rear legs. In particular, 12 DOF are actuated (α and β joints in front and middle legs and α and d joints in rear legs).

1) Horizontal walking: During horizontal walking the robot exhibited good stability properties. In Figs. 7, 8 and 9 the measured torques and forces at the coxa, femur and tibia joints are shown for a typical horizontal walking . Torques are measured in Kgf · cm, while forces are measured in N. The maximum (absolute) value for the torques is $\mu_{max} \simeq 4.5$ Kgf · cm and the maximum (absolute) value for the forces is $f_{max} \simeq 3.5$ N. These values are in the foreseen range. Considering a step frequency of 0.5 Hz, Gregor I walking speed (measured as body length per second) is $v \simeq 0.15$.
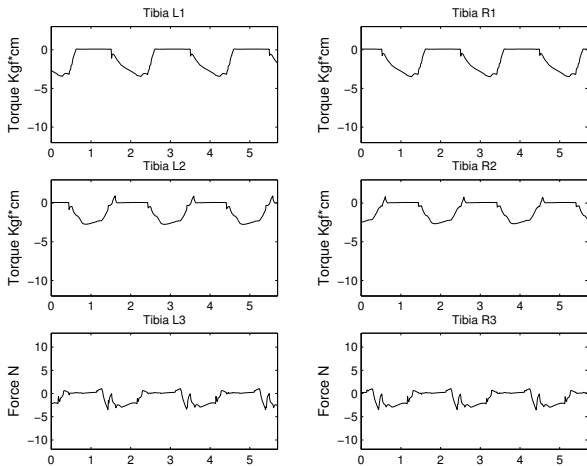
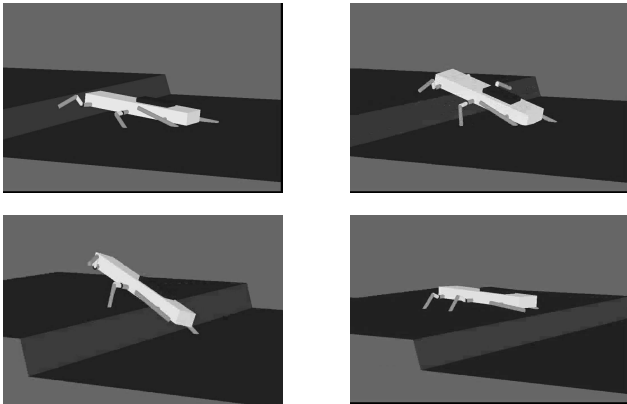Fig. 9. Tibia torques and forces during walking (on the x-axis time in seconds is shown).

Fig. 10. Climbing a 6 cm (150 % of robot CoM height) obstacle.

2) Obstacle climbing: We can gain more insights into the efficiency of the proposed structure by simulating the robot during obstacle climbing. Several simulations showed that thanks to the particular leg-body articulation and, above all, to the linear piston-like actuation of rear legs, Gregor I is able to overcome obstacles even beyond its CoM height (up to 8 cm, *i.e.* up to 200% of robot height) without any postural adjustment. This result proves the high stability of the overall structure and the efficiency of rear leg thrust. In Fig. 10 some snapshots of Gregor I climbing a 6 cm obstacle are shown. It is worth noticing how the rear legs propel the robot forward.

The maximum (absolute) value for the torques is $\mu_{max} \simeq 4.9$ Kgf $\cdot$ cm and the maximum (absolute) value for the forces is $f_{max} \simeq 12$ N. As expected, rear legs have to provide higher forces.

3) Maximum payload: Finally, we determined maximum achievable payload, during walking phase, in presence of motors able to deliver a maximum torque $\mu = 11$ Kgf $\cdot$ cm. The maximum payload that the robot can carry during horizontal walking is $\Pi = 2.5$ Kg.

VI. PHYSICAL IMPLEMENTATION

We have built an experimental platform (Fig. 13) as an instantiation of the design concepts of Section III-IV and the simulation results of Section V. Robot hardware implementation will be described in detail in a forthcoming paper ([20]), with a particular emphasis on the circuitry. Here we just describe the main features and the preliminary results.

A. Mechanical structure

The main body is 30 cm long, 9 cm wide and 4 cm high; the body is simply made of two aluminium sections joined by two threaded bars. This simple structure can accomodate both onboard electronics and batteries.

To ease the implementation, in this prototype we considered middle legs structurally and kinematically identical to front legs. For rear leg tibia segments a conversion mechanism from rotational motion to linear motion and a piston mechanism have been adopted; moreover the rotation axis of the rear coxa joint has been shifted in order to avoid an excessive stress on the motor axis, as shown in Fig. 11. Each leg segment is made of hollow aluminum tubes.

Segment physical dimensions and joint excursions are very close to those of the model described in section III. Joints α and β in front and middle legs and joints α and d in rear legs (12 joints overall) are directly actuated by 12 servos Hitec HS-945MG delivering a stall torque of 11 Kgf $\cdot$ cm and weighing 50 g.

Fully assembled Gregor I weighs 1.2 kg; with respect to the bottom of the body, front part is 7 cm high and rear part is 1 cm. CoM is 5 cm high and pitch angle is 20 degrees as desired; thus, Gregor I, shown in Fig. 13, exhibits a sprawled posture.

B. Control architecture

All the computational and motor control hardware is on board, while the power supply is external; anyway, we plan to make soon Gregor I totally autonomous. The control architecture is made of a CNN-CPG chip (described in detail in [8]), two amplification stages, two PIC 18F2320 and, finally, two buffering stages. The CNN-CPG chip, made of six two-layer CNN cells, generate the twelve signals needed for locomotion. These signals firstly undergo
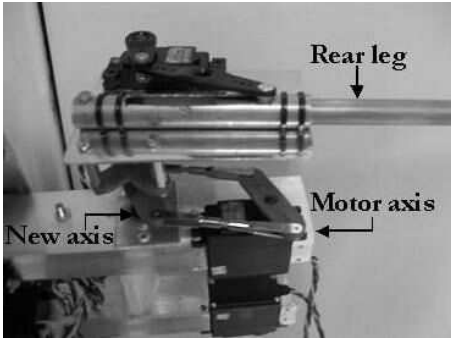
Fig. 11.   Rear leg.

an amplification stage based on TL914 operational amplifiers. Then they are converted by PIC in PWM signals (needed for motor control) and buffered. The overall architecture is shown in Fig. 12.
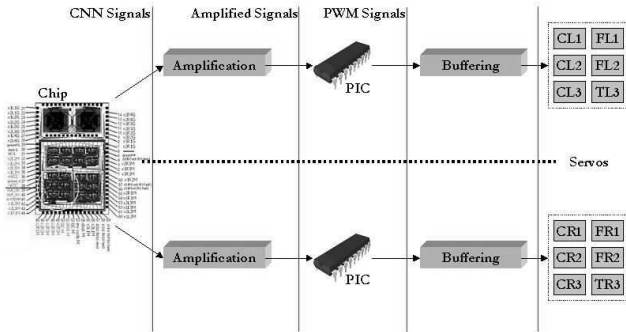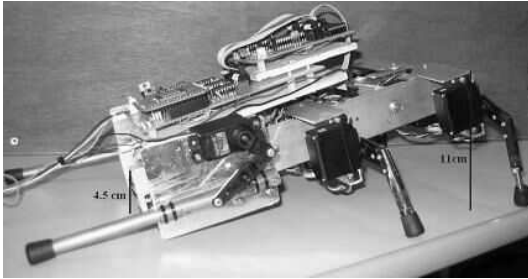

Fig. 12.   Control architecture.

Fig. 13.   Gregor I.

C. *Experiments*

Preliminary experiments have been performed to assess walking speed, obstacle climbing capabilities and energetic performance. We will use as a comparison robot RHex, since it is well documented and shows outstanding locomotion properties.

1) Speed: Speed has been measured simply relying on a chronometer and a rule and considering a step frequency of 0.5 Hz. Gregor I travels at the acceptable speed of 3 cm/s, *i.e.* 0.1 body length per second. Gregor I speed is substantially in accordance with the simulation results provided previously.

2) Obstacle crossing: Obstacle climbing capabilities of Gregor I were evaluated with two different obstacles. Firstly an obstacle 8.5 cm high, *i.e.* 170% of robot CoM height or 121% of front part height, was considered: over several trials the robot was always able to surmount it. Then, we tested Gregor I over a composite obstacle with a maximum height of 12.5 cm, *i.e.* 250% of robot CoM height or 178% of front part height; obstacle was overcome successfully.

As a comparison, RHex is able to negotiate obstacles with height 130% of front part height, while Sprawlita is able to negotiate obstacles with height 100% of front part height. Therefore Gregor I exhibits excellent obstacle climbing capabilities.

To demonstrate Gregor I rough terrain capabilities, we constructed an obstacle course made of 7 randomly spaced obstacles between 2 and 4 cm high (that is, between 28.5% and 57% of front part height and exceeding ground clearance between 1 and 3 cm). Over 10 runs, 9 runs were successful, while in one run Gregor I broke one leg.

3) Energetic performance: Power consumption ranges between 15 W during walking on even terrain and 25 W during obstacle climbing.

To measure energy efficiency we use the "Specific Resistance" ε [21]:

$$\varepsilon = P/(mgv)$$

based on the robot's weight, mg, and its average power consumption, P, at a particular speed, v. Specific Resistance is increasingly popular and can be used to compare vehicles regardless of size, speed or configuration.

The specific resistance was lowest on even terrain, $\epsilon = 42$, and highest during obstacle course, $\epsilon = 70$. As a comparison, RHex Specific Resistance ranges between $\varepsilon = 2.5$ and $\varepsilon = 14$. Therefore energy efficiency of Gregor I is, for now, very low and needs to be improved.

VII. Conclusions

A novel structure and control system architecture for an hexapod robot have been proposed. Both structure and locomotion control are inspired by biological observations in cockroaches.

Our major concern was on the implementation of rear legs, that seem to play a crucial role in obstacle overcoming and payload capability, and on

the locomotion control, performed in this work by a Cellular Neural Network (CNN) playing the role of an artificial Central Pattern Generator (CPG).

Preliminary experiments with the robot are encouraging: Gregor I is able to walk at the travel speed of 0.1 body length per second and to successfully negotiate obstacles whose height is equal to the 120% of front part height – a good results if compared to the performance of other hexapod robots.

Moreover, the CNN-CPG approach has been shown to be suitable for the locomotion control of legged robots equipped with legs with different and complex design. This approach provides modularity, robustness, flexibility and ease of implementation; furthermore, since it just relies on analog circuitry, it seems to be particularly robust against space radiation and thus qualified for space applications.

VIII. ACKNOWLEDGMENTS

REFERENCES

[1] D. Kingsley, R. Quinn, and R. Ritzmann. *A cockroach inspired robot with artificial muscles.* Proc. of International Symposium on Adaptive Motion of Animals and Machines (AMAM), Kyoto, Japan, 2003.

[2] L. H. Ting, R. Blickhan And R. J. Full. *Dynamic And Static Stability In Hexapedal Runners.* J. exp. Biol., 197, pp. 251–269, 1994.

[3] G.M. Shepherd *Neurobiology*. Oxford University Press, Oxford, 1994.

[4] P. Arena, L. Fortuna, and M. Frasca, *Multi-template approach to realize central pattern generators for artificial locomotion control* Int. J. Circ. Theor. Appl., vol. 30, pp. 441458, 2002.

[5] L. O. Chua and L. Yang. *Cellular neural networks: Theory.* IEEE Trans. Circuits Syst. I, 35, pp. 1257–1272, 1988.

[6] M. Frasca, P. Arena, L. Fortuna. *Bio-Inspired Emergent Control Of Locomotion Systems.* World Scientific Series on Nonlinear Science, Series A - Vol. 48, 2004.

[7] P. Arena, L. Fortuna, M. Frasca, L. Patané, G. Vagliasindi. *CPG-MTA implementation for locomotion control.* Proc. of IEEE International Symposium on Circuits and Systems, Kobe, Japan, May 23-26, 2005.

[8] P. Arena, S. Castorina, L. Fortuna, M. Frasca, and M. Ruta *A CNN-based chip for robot locomotion control.* Proc. ISCAS03, 2003.

[9] www.eas.asu.edu/ holbert/eee460/see.html

[10] R. D. Quinn and R. E. Ritzmann. *Construction of a hexapod robot with cockroach kinematics benefits both robotics and biology.* Connect. Sci., 10, No. 3-4, pp. 239–254, 1998.

[11] F. Delcomyn and M. E. Nelson. *Architectures for a biomimetic hexapod robot.* Robotics and Autonomous Systems, 30, pp. 5–15, 2000.

[12] J. E. Clark, J. G. Cham, S. A. Bailey, E. M. Froehlich, P. K. Nahata, R. J. Full, M. R. Cutkosky. *Biomimetic Design and Fabrication of a Hexapedal Running Robot.* Proc. of IEEE International Conference on Robotics and Automation, 2001.

[13] J. T. Watson, R. E. Ritzmann, S. N. Zill and S.J. Pollack. *Control of obstacle climbing in the cockroach,* Blaberus disoidalis*, I. Kinematics.* J. Comp. Physiol. A., 188, pp. 39–53, 2002.

[14] H. Ritter, T. Martinetz and K. Schulten. *Neural Computing and Self-Organizing Maps Reading.* MA: Addison-Wesley, 1992.

[15] U. Saranli, M. Buehler, D. E. Koditschek. *RHex: A Simple and Highly Mobile Hexapod Robot.* The International Journal of Robotics Research Vol. 20, No. 7, pp. 616-631, 2001

[16] www.ai.mit.edu/projects/boadicea/boadicea.html

[17] M. Pavone. *Mathematical models for biomimetic solutions in aerospace engineering.* M.Sc. Thesis, 2004.

[18] S. McMillan, D. E. Orin and R. B. McGhee. *A computational framework of underwater robotic vehicle systems.* J. Auton. Robots - Special Issue On Autonomous Underwater Robots, 3, pp. 253–268, 1996.

[19] P. Arena, L. Fortuna, M. Frasca and G. Sicurella. *An Adaptive, Self-Organizing Dynamical System for Hierarchical Control of Bio-Inspired Locomotion.* IEEE Transactions On Systems, Man, And Cybernetics Part B: Cybernetics, 34, No. 4, pp. 1823–1837, 2004.

[20] P. Arena, L. Fortuna, M. Frasca, L. Patan, M. Pavone. *Implementation and experimental validation of an autonomous hexapod robot.* To be submitted to Proc. of IEEE International Symposium on Circuits and Systems, Kos, Greece, May 21-24, 2006.

[21] G. Gabrielli and T. H. von Karman,*What price speed?.* Mechanical Engineering, vol. 72, no. 10, pp. 775781, 1950.